Mediterranean Marine Science

Vol 22, No 3 (2021)

VOL 22, No 3 (2021)

A three dimensional, full life cycle, anchovy and sardine model for the North Aegean Sea (Eastern Mediterranean): Validation, sensitivity and climatic scenario simulations

ATHANASIOS GKANASOS, EUDOXIA SCHISMENOU, KOSTAS TSIARAS, STYLIANOS SOMARAKIS, MARIANNA GIANNOULAKI, SARANTIS SOFIANOS, GEORGE TRIANTAFYLLOU

doi: 10.12681/mms.27407

Research Article

Mediterranean Marine Science
Indexed in WoS (Web of Science, ISI Thomson) and SCOPUS
The journal is available on line at http://www.medit-mar-sc.net
DOI: http://doi.org/10.12681/mms.27407

A three dimensional, full life cycle, anchovy and sardine model for the North Aegean Sea (Eastern Mediterranean): Validation, sensitivity and climatic scenario simulations

Athanasios GKANASOS[1,2], Eudoxia SCHISMENOU[3], Kostas TSIARAS[2], Stylianos SOMARAKIS[3], Marianna GIANNOULAKI[3], Sarantis SOFIANOS[1] and George TRIANTAFYLLOU[2]

[1] Department of Environmental Physics, University of Athens, 15784 Athens, Greece
[2] Hellenic Centre for Marine Research (HCMR), Athens-Sounio Avenue, 19013 Anavyssos, Greece
[3] Hellenic Centre for Marine Research (HCMR), Thalassocosmos Gournes, Heraklion, Crete, Greece

Corresponding author: gt@hcmr.gr

Contributing Editor: Konstantinos TSAGARAKIS

Received: 2 July 2021; Accepted: 10 September 2021; Published online: 10 October 2021

Abstract

We present the development of a 3D full-lifecycle, individual-based model (IBM) for anchovy and sardine, online coupled with an existing hydrodynamic/biogeochemical low-trophic level (LTL) model for the North Aegean Sea. This IBM was built on an existing 1D model for the same species and area, with the addition of a horizontal movement scheme. In the model, both species evolve from the embryonic stage (egg+yolk sac larva) to the larval, juvenile, and adult stages. Somatic growth is simulated with the use of a "Wisconsin" type bioenergetics model and fish populations are computed considering reproduction and mortality (natural, fishing, starvation), along with an adaptation of the 'super individuals' (SI) approach. The 2000-2010 period was selected for the reference simulation and model calibration, in terms of fish growth and population biomass. The interannual biomass variability of anchovy was successfully represented by the model, while the simulated biomass of sardine exhibited low variability and did not satisfactorily reproduce the interannual variability observed in acoustic surveys. The spatial biomass distribution of both species was in relatively good agreement with field data. Additional single-species simulations revealed that species compete for food resources. Temperature sensitivity experiments showed that both species reacted negatively to a temperature increase. Anchovy, in particular, was more affected since its spawning and larval growth periods largely overlap with the period of maximum yearly temperature and low prey concentration. Finally, simulation experiments using IPCC climatic scenarios showed that the predicted temperature increase, and zooplankton concentration decrease will negatively affect anchovy, resulting in sardine prevalence.

Keywords: Anchovy; sardine; 3D full-life-cycle IBM; resource competition; climatic change.

Introduction

Small pelagic fish play a key role in marine food webs, being the trophic link between plankton and larger fish (Fréon *et al*., 2005). They are characterized by a short life and high fecundity, which result in pronounced sensitivity to environmental changes and significant variability in their abundance. In the Mediterranean Sea, anchovy (*Engraulis encrasicolus*) and sardine (*Sardina pilchardus*) are the most abundant small pelagic fish species. They are mainly found in the Gulf of Lions, the Straits of Sicily and the Alboran, Catalan, Adriatic, and North Aegean Seas. These regions provide suitable habitats for small pelagic fish, characterized by enhanced food availability, increased larval retention and, consequently, largely overlapping spawning and nursery grounds (Somarakis *et al*., 2019). However, changes in oceanographic conditions may affect differently the two species, since anchovy and sardine spawn and recruit in different seasons: Sardine mainly spawns during autumn and winter, whilst anchovy spawns in spring and summer (Somarakis *et al*. 2019; Gkanasos *et al.,* 2019).

Long-term changes in the environmental conditions of the Mediterranean Sea have already been documented (Skliris *et al*., 2011a, b); these may cause ecosystem shifts and changes in fisheries productivity (e.g., Tzanatos *et al*. 2013). Most anchovy and sardine stocks in the Mediterranean have shown declining trends in recent years (e.g., Tsikliras *et al*., 2015; Vilibić *et al*., 2016). There is also evidence of decreasing size and somatic condition due to increasing temperature and reduced plankton productivity (Brosset *et al*., 2015). In other studies (Tzanatos *et al*., 2013; Stergiou *et al.,* 2016), an opposite relationship with temperature for anchovy (positive) and sardine (negative) has been identified. Moreover, long-term variability in landings of Mediterranean anchovy and sardine reveal

fluctuations connected to environmental factors (Voulgaridou & Stergiou, 2003). In the Aegean and Ionian Seas, limited food resources lead to increased inter- and intra- species competition (Katara *et al*., 2011), while an analysis of catch data has shown that both species have a negative relationship with increasing temperature, being stronger for sardine (Katara *et al*., 2011).

End-to-end models have been introduced (Travers *et al*., 2007) for the study of ecosystem dynamics, integrating the physical and biological processes of different trophic levels in the marine environment, from nutrients to primary production and from zooplankton to pelagic fish. Such models have been implemented successfully for anchovy and sardine in the California Current (Rose *et al.,* 2015) and for the Canary Current ecosystem (Sánchez-Garrido *et al.,* 2019). Politikos *et al*. (2015) developed a 3-D individual based model (IBM), describing the full-life cycle of anchovy in the N. Aegean, while Gkanasos *et al.* (2019) extended the existing anchovy model to a 1-D multispecies (anchovy and sardine) model for the N. Aegean.

In this study, a 3-D hydrodynamic/biogeochemical model was coupled online with a full-life cycle IBM, describing the dynamics and spatial distribution of both anchovy and sardine stocks in the North Aegean Sea. The N. Aegean is a marginal Sea, connecting the eastern Mediterranean and Black Sea basins (Fig. 1). Nutrient inputs from local rivers and Black Sea Water (BSW) discharge at the Dardanelles straits contribute to enhanced plankton productivity (Frangoulis *et al.,* 2010; Siokou-Frangou *et al*., 2002). The previous implementation of a 1-D model (Gkanasos *et al*., 2019) was particularly useful for setting up the main attributes of the dynamics of the two species, despite its limitation in resolving horizontal processes. In this study, a more realistic description of the dynamics is provided, using a 3-D spatially explicit model that includes the spatial variability induced by fish movement and egg/larval advection by ocean currents. The simulated model output was validated against available data relating to larval growth, weights-at-age and estimated biomasses obtained from acoustic surveys, for both species.

Most climate change scenarios suggest that the most probable change will be an increase of atmosphere and sea temperature (Sarmiento *et al.,* 1998). Such an increase would affect the metabolic processes of fish, as well as plankton production and prey availability. On that basis, a series of sensitivity experiments were performed in this study, to gain a better understanding of the effect of changing temperature on fish growth and biomass. Moreover, as the two species share the same zooplankton resources, sensitivity experiments were performed to identify their potential interaction through resource competition. Finally, the impact of climate change, affecting both temperature and food availability, on the two species was investigated by running two simulations, under two sets of climatic conditions, "present" (1980-2000) and "future" (2080-2100).

Materials and Methods

Model Description

Low-trophic level model

The coupled low-trophic level (LTL) model consists of the hydrodynamic model, which is based on the Princeton Ocean Model (POM; Blumberg & Mellor, 1983) and the biogeochemical model, based on the European Regional Seas Ecosystem Model (ERSEM, Baretta *et al*. 1995). The hydrodynamic model is a primitive equation, free-surface, sigma coordinate circulation model that provides the fields of temperature, salinity, and ocean currents, as well as the coefficients of horizontal and vertical

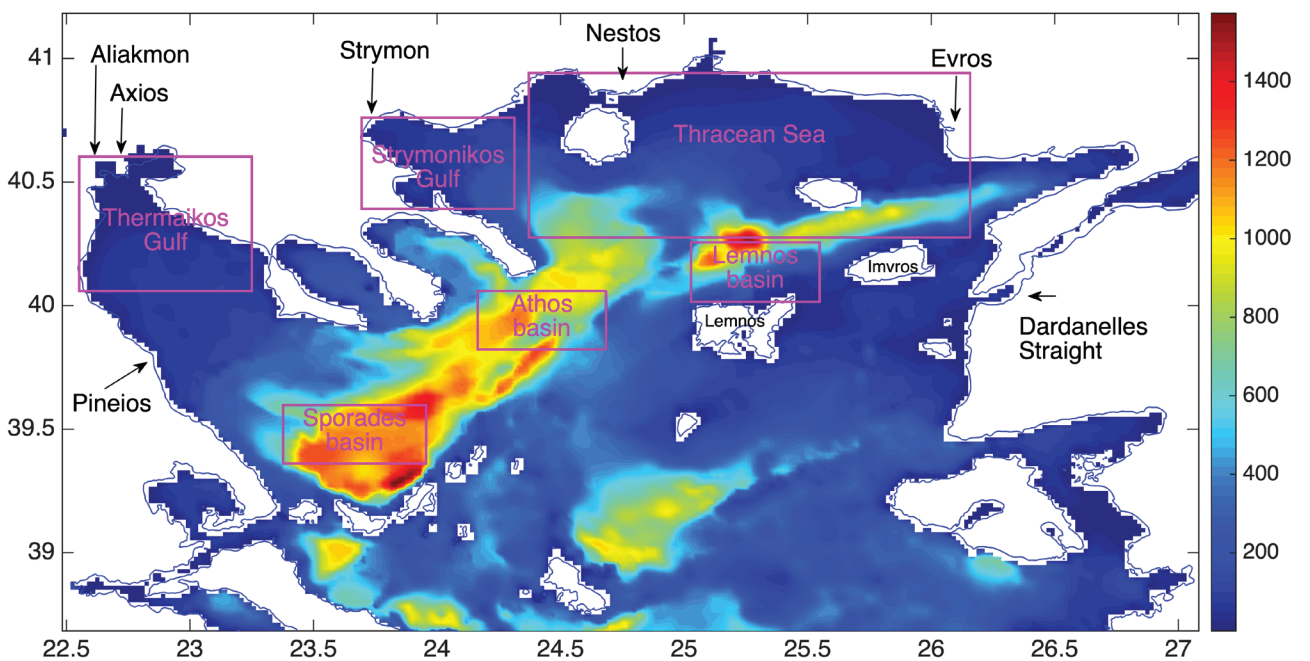

Fig. 1: North Aegean Sea bathymetric map (depth in meters). Major rivers are also indicated.

mixing. POM forces the biogeochemical ERSEM model; in ERSEM, the organisms are classified according to their trophic role (consumers, producers, etc.) and size, according to the functional group approach. The planktonic food web consists of bacteria, picophytoplankton, nanophytoplankton, diatoms, dinoflagellates, heterotrophic nanoflagellates, microzooplankton and mesozooplankton. The model also includes dissolved inorganic nutrients (phosphate, nitrate, ammonium, silicate) and pools of particulate and dissolved organic matter. Each plankton group has dynamically varying C:N:P:Si pools. Hence, the nitrogen, phosphorus and silicate cycles are coupled with carbon dynamics. The coupled model has been implemented in the Cretan Sea (Petihakis *et al*., 2002), the North Aegean Sea (Tsiaras *et al*., 2012; 2014; Petihakis *et al.*, 2014; Politikos *et al*., 2015; Chust *et al*., 2014) and is currently operational at Mediterranean basin scale (Kalaroni *et al*., 2020), as part of the POSEIDON forecast system (www.poseidon.hcmr.gr).

Fish IBM

A 3-D IBM was developed for the North Aegean Sea ecosystem, aiming to describe the full life cycle of anchovy and sardine (from egg to adult), their spatial distribution and their important energetic features. For computational efficiency, anchovy and sardine populations are grouped into super individuals (SI) (Scheffer *et al.,* 1995); each SI consists of individuals that share the same properties, such as life stage/age class, weight (g), length (mm), age (days) and position (longitude, latitude). SIs that belong to the same life stage or age class have identical characteristics in terms of feeding preferences, mortalities and movement. In order to prevent the total number of SIs from continuously increasing after each spawning cycle, when that number exceeds a certain limit, SIs of the same age class found within a predefined distance are merged and their properties averaged.

Anchovy lifespan is divided into seven stages and sardine lifespan into eight stages. These include the embryonic stage, the early and late larval stages, the juvenile stage and the adult life stages; there are three anchovy age classes for anchovy and four sardine age classes. The duration of the embryonic stage (egg+yolk sac larva) is temperature-dependent and regulated by the equations developed by Gatti *et al.* (2017). Subsequently, the stage transition is length-dependent until the juvenile stage and after that it is based on calendar criteria (Table 1).

Bioenergetics

Fish growth is calculated with a Wisconsin-type bioenergetics model, taking into account all significant processes, such as consumption, respiration, egestion, excretion, specific dynamic action and reproduction. Somatic growth is regulated through the following equation:

$$\frac{1}{W_{SI}} \cdot \frac{dW_{SI}}{dt} = [C - (R + EG + SDA + EX + E_{buffer})] \cdot \frac{CAL_z}{CAL_f}$$

where W_{SI} corresponds to fish wet weight (g), t to time (days), C to consumption, R to respiration, EG to egestion, SDA to specific dynamic action, EX to excretion, E_{buffer} to the energy allocated to reproduction, CAL_z to the caloric equivalent of zooplankton and CAL_f to the caloric equivalent of fish. The equations and parameters of the individual functions are thoroughly described in Gkanasos *et al*. (2019). Briefly, consumption is a func-

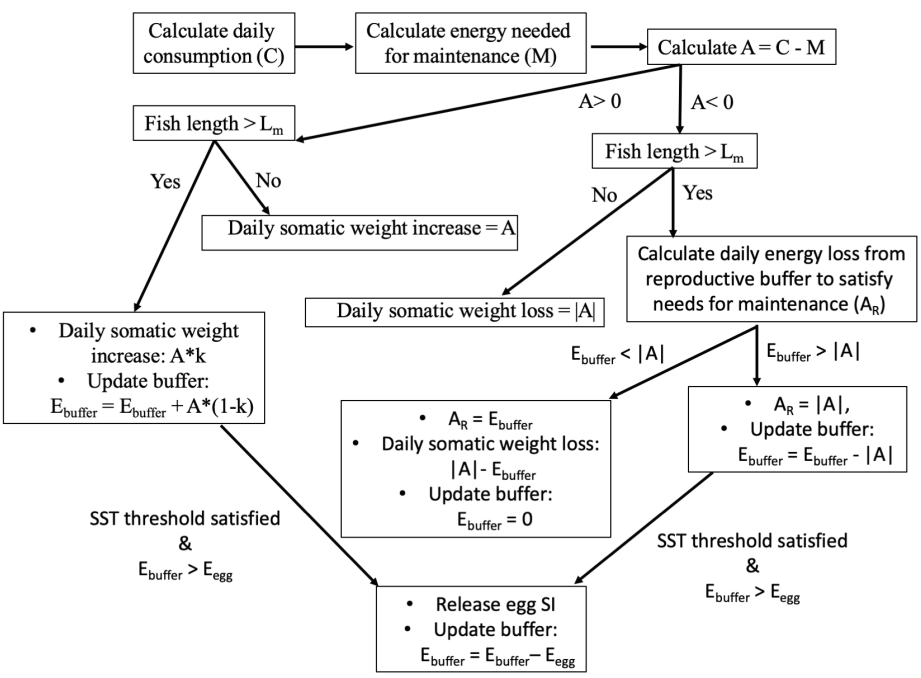

Fig. 2: Schematic illustration of the energy allocation and egg production algorithm. SST: Sea surface temperature. L_m: length at maturity. E_{buffer}: energy in reproduction buffer. E_{egg}: batch energy (Gkanasos *et al*., 2019).

Table 1. Anchovy and sardine model parameters.

Parameter	Anchovy	Sardine
[a] Length range (mm):		
Early larvae	4-11	5-13
Late larvae	11-42	13-50
Juvenile	42-100	50-105
Adult Stage, age-1	5th March – 4th March (year+1)	1st September – 3th August(year+1)
Adult Stage, age-2	5th March – 4th March (year+1)	1st September – 3th August(year+1)
Adult Stage, age-3	5st March – 1stDecember	1st September – 3th August(year+1)
Adult Stage, age-4	-	1st September – 30th April(year+1)
[a] Length at maturity (Lm, mm)	100	105
[b] Egg energy	0.66	1.11
[c] Daily specific fecundity (eggs g-1)	46	20.1
Batch Energy (g prey per g fish per day)	0.012	0.0086
[d] Spawning period SST threshold	Start: SST >15°C End: October	Start: SST <16°C End: mid-April
Optimum temperatures for consumption	18 (early larvae) 15.85 (late larvae) 15.1 (juveniles/adults)	14.2 (early larvae) 14.2 (late larvae) 15.1 (juveniles/adults)
Half saturation parameters for consumption	0.12 (early larvae) 0.08 (late larvae) 0.14 (juveniles) 0.205 (adults age 1) 0.175 (adults age 2) 0.272 (adults age 3)	0.17 (early larvae) 0.15 (late larvae) 0.0975 (juveniles) 0.157 (adults age 1) 0.19 (adults age 2) 0.19 (adults age 3) 0.2 (adults age 4)
[e] Natural mortalities	0.4, embryos 0.2, early larvae 0.05, late larvae 0.012, juveniles* 0.002, adults	
[e] Fishing mortalities (adults)	0.00136	0.002

[a] Schismenou (2012), [b] Gatti *et al*. (2017), [c] Somarakis *et al.* (2012), Ganias *et al.* (2014), [d]Somarakis (1999), Tsikliras (2007), [e]Politikos (2015), Antonakakis *et al.* (2011), Giannoulaki *et al.* (2014).
*The natural mortality of juveniles was calibrated (see text for details).

tion of prey density and its assimilation rate, respiration is a weight-dependent function, egestion, specific dynamic action, and excretion emerge from consumption, while any surplus energy is directed to growth in immature fish or to both growth and reproduction in adult fish (see Appendix and Table 2 in Gkanasos *et al.,* 2019).

Movement

Egg and early larval stages are considered as passive tracers (Huret *et al.,* 2010) in the model, and their movement is governed by the hydrodynamic circulation. They are assumed to remain in the upper 30 meters of the water column (Politikos *et al.,* 2015), with no vertical movement due to buoyancy. Late larvae, juveniles and adult stages are assumed to perform diurnal vertical migration between the surface layer (0-30 m) during the night and the sub-surface layer (>30m) during the day. Horizontally, fish are assumed to move towards areas with higher food availability, exploiting ocean currents in order to move in the desired direction (for more details, see Politikos *et al.,* 2015). The maximum swimming speed is assumed to be proportional to fish length. A random component is

Table 2. Simulated species annual mean biomasses (in parentheses: simulated biomass during June) and mesozooplankton concentration in single and multispecies experiments.

	Two-species	Single species	
		anchovy	sardine
Anchovy biomass (kt)	45 (59)	47 (61)	-
Sardine biomass (kt)	11.5 (19)	-	42 (60)
Total biomass (kt)	56.5	47	42
Mesozooplankton concentration (0-100m) (mgC/m^3)	1.93	1.95	2.12

also included in fish movement, as well as a function of bathymetry to keep adult and juvenile fish from moving towards very deep waters (>300m) or close to the coastline, based on existing knowledge of fish habitats in the N. Aegean Sea (Giannoulaki *et al*., 2005).

To prevent overcrowding in areas with high zooplankton concentration, fish movement takes into account the fish density in surrounding cells. This is achieved using a "food per capita" gradient, calculated from the ratio of available zooplankton over the fish biomass in neighboring cells. SIs move towards cells with higher food per biomass concentration as long as this is sufficient for the fish in the cell (i.e., no weight loss is caused). In such cases, the aforementioned criterion is bypassed, and SIs are simply directed to neighboring cells with higher food availability.

Population dynamics

The species population (N) is regulated by reproduction, as well as natural (M) and fishing (F) mortalities:

$$\frac{dN}{dt} = -(M + F) \times N$$

Fishing mortality is applied only to the adult stages (Giannoulaki *et al*., 2014; Gkanasos *et al*., 2019). The anchovy fishing grounds in the North Aegean Sea mainly include the continental shelf areas of the Thermaikos Gulf, Thracian Sea and Strymonikos Gulf (Fig. 1). The natural mortalities adopted are the same as in Gkanasos *et al*. (2019) and are stage-specific (Table 1) for both sardine (Antonakakis *et al*., 2011) and anchovy (Politikos *et al*., 2015; Giannoulaki *et al*., 2014). For the juvenile stages, the adopted natural mortality is based on stock assessment estimates and was treated as a calibrated parameter in order to achieve a best fit with the field biomass estimates.

Finally, for fish found in unfavourable conditions, a cumulative weight loss of more than 35% of body weight is assumed to cause mortality due to starvation. This limit was set empirically after examining the available length-weight relationships of larvae, juveniles, and adults (see Politikos *et al.,* 2015). In all cases, residuals of the length-weight relationship were <35% of predicted weight.

Reproduction

An energy allocation algorithm, regulating the energy reserves of fish, controls the spawning process (for details, see Gkanasos *et al*., 2019). In adult fish, after satisfying maintenance needs (i.e., respiration, egestion, specific dynamic action, and excretion), a percentage (k) of the surplus energy (A) is channelled to somatic weight increase (growth), and the remaining $A \times (1 - k)$ is channelled to a 'reproductive buffer' in order to be used either for reproduction or for maintenance in cases of deficient food availability.

In the Mediterranean Sea, the two species have different reproductive periods: sardine spawns during autumn and winter and anchovy during spring and summer. In past studies (Ganias *et al*., 2007; Somarakis *et al*., 2019), sardine was reproductively active from November to April and anchovy from May to September. Therefore, a combination of temperature and calendar day criteria was adopted to define the spawning periods of the two species. Anchovy spawns when SST is above 15 °C and until the end of September, while sardine starts to spawn when SST falls under 16 °C and continues until mid-April. During this period, eggs are released daily; total batch energy (Total E_{egg}) is derived from daily specific fecundity (DSF, number of eggs released per gram of adult SI), the weight of SIs and the egg energy of each species (Gatti *et al.,* 2017).

Coupling with the LTL model

The LTL model and the fish IBM are two-way, dynamically coupled. Both anchovy and sardine consume zooplankton: early larvae consume microzooplankton, late larvae consume both micro and mesozooplankton with an equal preference, while juveniles and adults feed only on mesozooplankton (Morote *et al*., 2010; Nikolioudakis *et al*., 2011). The heterotrophic biomass (microzooplankton, mesozooplankton) consumed by the fish was removed in the LTL model, while fish by-products are fed back into the LTL model. Fluxes due to fish egestion and specific dynamic action are channelled to the organic particulate (detritus) matter pool of the LTL and fluxes due to excretion return as dissolved organic matter (for more details, see Politikos *et al*., 2015). Moreover, individual fish within each SI that perform vertical migration

(late larvae, juveniles, and adults) are assumed to have a vertical distribution that is closely related to maximum prey availability. Based on that assumption, the fluxes in terms of zooplankton consumption, as well as released inorganic nutrients and organic matter are calculated for each depth and applied to the LTL model (for more details, see Politikos *et al*., 2015).

Model simulations setup

Reference simulation

A long-term hindcast simulation was performed over the 2000-2009 period. The atmospheric forcing was obtained from HIRHAM model re-analysis (Christensen *et al*., 1996). Initial fields and open boundary conditions for the biogeochemical and hydrodynamic models were obtained from a Mediterranean basin scale model simulation over the 2000-2009 period (Kalaroni *et al*., 2020). The coupled model was initially integrated for a 5-year spin-up period. Mean (1995 – 1999) river nutrient load data for major N. Aegean rivers (Evros, Axios, Aliakmonas, Strymon, Pinios, Nestos, see Figure 1) were obtained from Skoulikidis (2009). The Dardanelles water exchange was parameterized using a two-layer (inflow of BSW and outflow of Aegean water) open boundary condition (Nittis *et al*., 2006), with seasonally varying concentrations of dissolved inorganic nutrients (Tuğrul *et al*., 2002) and annual mean concentrations of ammonium, dissolved and particulate organic matter (Polat & Tuğrul, 1996). A phytoplankton input was also adopted, based on a monthly climatology of available SeaWiFS (Sea-viewing Wide Field-of view Sensor) Chl-a data (O'Reilly *et al*., 1998).

The fish model was initialized on 1st January 2000, as in Politikos *et al*. (2015), taking into account the biomass of each species mean, as estimated from acoustic surveys, and their main habitat areas (Giannoulaki *et al.,* 2014) in Thermaikos Gulf, Strymonikos Gulf, the Thracian Sea and the BSW inflow area, east of Limnos Island (see Fig. 1). An initial number of 1000 SIs was assigned, for each of three anchovy (juveniles, age-1, age-2) and four sardine (juveniles, age-1, age-2, age-3) age classes, with reference weights per age.

Resource Competition

In order to study the effect of trophic competition, a series of simulations were performed. These included single and two species model setups, starting with reference or inverted initial biomasses; the latter can provide insight into species acclimatization in the area. The variability of zooplankton exploitation in either one or two species experiments was also investigated.

Temperature sensitivity experiments

Temperature sensitivity experiments were run to gain a better understanding of the impact of increasing temperature on fish metabolism and biomass. Specifically, a series of 10-year (2000-2009) simulations were run, adopting a temperature increase (+1 ^{o}C and +2 ^{o}C) encountered by the fish (i.e., no change in the hydrodynamic and biochemical model) and affecting somatic growth, while the duration of the spawning period remained the same. To investigate whether the temperature effect on anchovy and sardine biomass was related with early life stage (i.e., larvae and juveniles) survival or changes in egg production, the temperature increase was applied separately on early (t. on earl.), adult (t. on ad.) and both early and adult life stages (t. on all st.). The potential interaction between the two species due to resource competition was also investigated by comparing the two-species reference and temperature sensitivity simulations with single-species reference and temperature sensitivity simulations, i.e., without any resource competition.

Climatic scenarios

Finally, two simulations were performed, adopting present (1980-2000) and future (2080-2100) climatic conditions under the IPCC-A1B scenario (Chust *et al*., 2014). The atmospheric forcing for these climate simulations was obtained from SINTEX-G (INGV-SXG, Gualdi *et al.*, 2008) fully coupled global atmosphere-ocean general circulation model. The open boundary conditions for the biogeochemical and hydrodynamic models were obtained from a Mediterranean basin scale model simulation over the same periods (Stergiou *et al*., 2016). Both river and BSW discharge and nutrient inputs were the same in the two simulations.

Results

Ecological Model

The average (2000 - 2009) near surface circulation and salinity, chlorophyll and mesozooplankton concentrations is presented in Figure 3. The model correctly simulates the main aspects of the circulation in the N. Aegean, as known from observational studies and previous modelling efforts (Kourafalou & Tsiaras, 2007; Tsiaras *et al*., 2012, 2014; Petihakis *et al*., 2015). A cyclonic circulation is simulated, driven by the inflow of Levantine water from the South and brackish BSW through the Dardanelles. The latter branches around Limnos Island, creating a semi-permanent anti-cyclone in the North East (Zervakis & Georgopoulos, 2002; Olson *et al.,* 2007), and transferring BSW to the South Aegean following a southwest pathway. An anti-cyclonic circulation is also simulated in the Sporades basin (Androulidakis & Kourafalou, 2011; Olson *et al*., 2007).

Phytoplankton concentration (Fig. 4) increases during

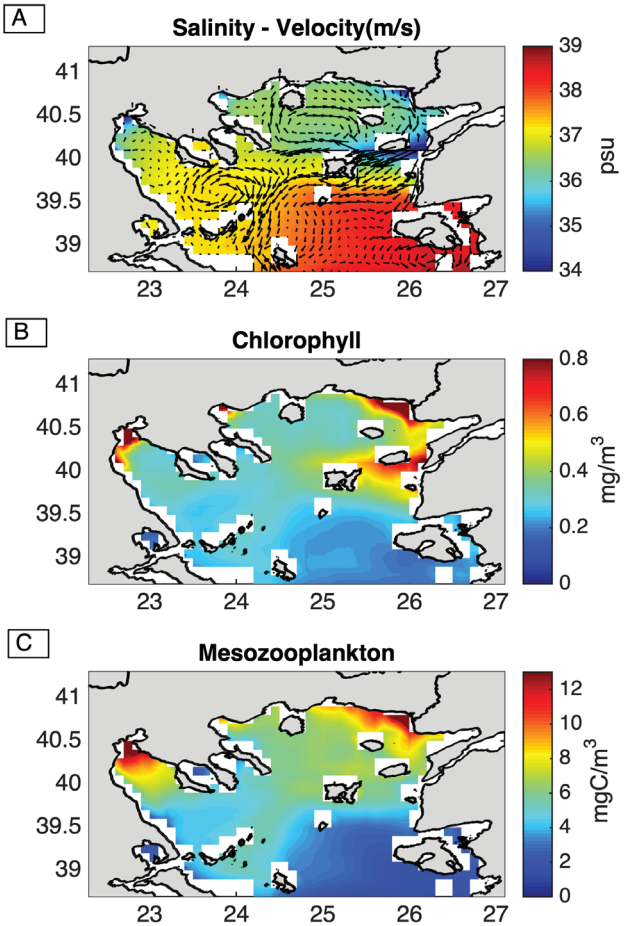

Fig. 3: Mean (2000-2009) simulated A) surface salinity (psu) & velocity (m/s), B) chlorophyll concentration (mg/m^3), C) mesozooplankton concentration (mgC/m^3).

winter-spring and peaks in March, following the entrainment of sub-surface nutrients from increased vertical mixing, and nutrient inputs from BSW and river runoff that peak over the same period. Mesozooplankton concentration, the main prey of anchovy/sardine, follows the phytoplankton bloom with a 1-2 months delay, peaking during April-May. Sea surface temperature increases in spring and peaks in August.

Anchovy-sardine fish model reference simulation and validation

The basic species attributes used for model calibration are the early and adult stage growth in terms of body length and weight respectively, as well as the seasonal evolution and spatial distribution of biomass and the production of eggs. The biomass and the weight/length -at-age data were obtained from acoustic surveys and field sampling respectively, performed from 2003 to 2008. Reference larval lengths were obtained from studies on anchovy and sardine conducted by Schismenou (2012) and Schismenou *et al.* (2013, 2016). It should be noted that acoustic biomass estimates include all fish >80 mm; therefore, the model derived biomasses include juveniles >80 mm as well as all adult stages.

Growth

The simulated mean growth trajectories were in good agreement with the field data both for larval (Fig. 5) and adults stages (Fig. 6). Anchovy and sardine adults gain more weight from winter to midsummer (July); this period coincides with the increased mesozooplankton concentration period.

Biomasses

Model derived biomass estimates (Fig. 7) were in partial agreement with acoustic biomass estimates; the model failed to capture the observed increasing trend in the biomass of sardine and the particularly high biomasses estimated in 2006 and 2008. Model-derived biomass estimates revealed two yearly anchovy peaks (in January

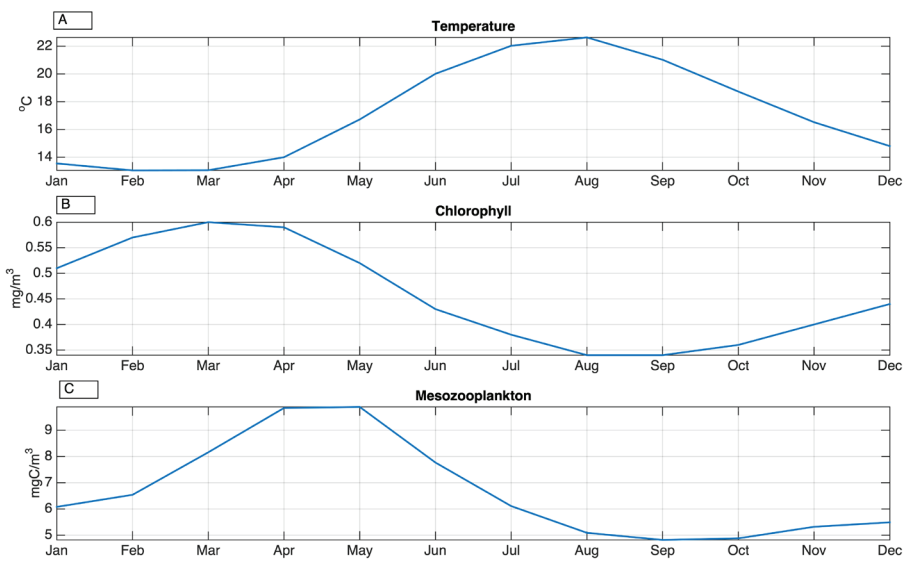

Fig. 4: Mean (2000-2009) seasonal evolution of A) simulated sea surface temperature (°C), B) chlorophyll (mg/m^3) and C) mesozooplankton biomass (mgC/m^3).

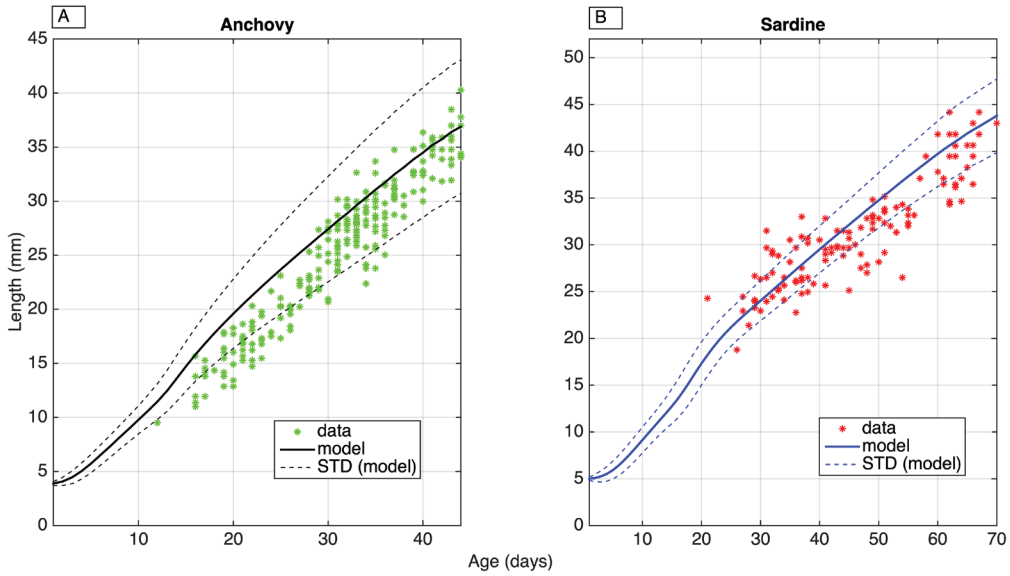

Fig. 5: Mean lengths (mm) at age (±SD) of A) anchovy and B) sardine larvae against field data

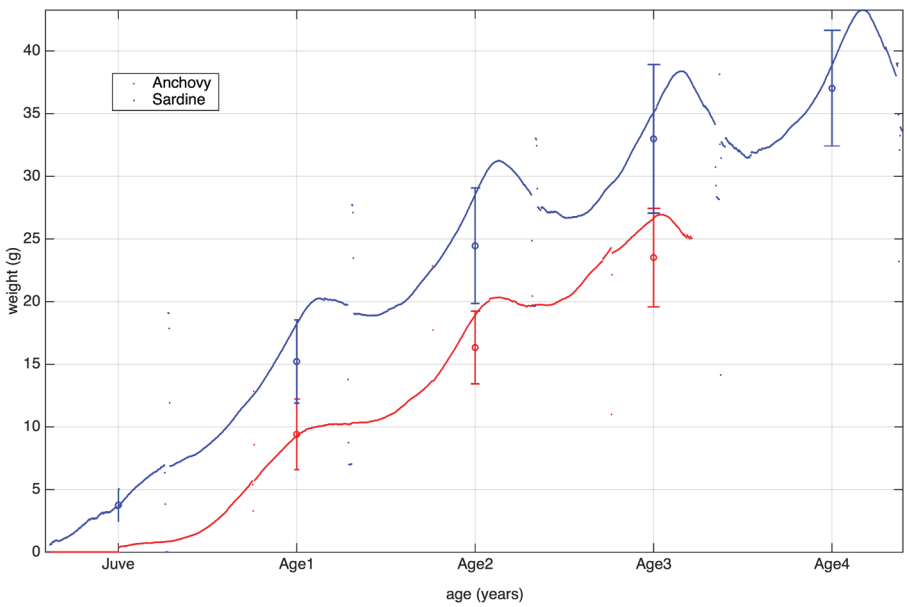

Fig. 6: Modelled mean weight (g) -at- age against field data (red & blue circles ±SD).

and in June); the first peak can be attributed to the recruitment of juveniles above 80 mm in length, while the second may be attributed to the optimum somatic condition of adults from April to July (Gkanasos *et al.,* 2019). On the other hand, sardine modelled biomass peaked during June-July, when increased juvenile abundance and optimum somatic condition coincide.

The simulated spatial distribution of biomass, for both species (Fig. 8), indicates high concentrations in Thermaikos Gulf, Strymonikos Gulf, and the Thracian Sea coastal areas (<100m), which is in good agreement with the literature (Giannoulaki *et al.,* 2005). These areas are characterized by high primary production and zooplankton concentration, associated with the BSW and river nutrients, as shown above (Fig. 3). However, the model failed to reproduce the observed high biomass patches east of Limnos Island. This could be due to an overestimated BSW-induced current that may result in offshore advection of eggs/larvae. Indeed, the simulated sea surface velocities in the area between Limnos and Imvros Islands were higher compared to those derived from HF Radar observations (Kokkini *et al*., 2014)

Egg production

The simulated sardine egg production increases slowly from November to March and sardine reproduction ceases in mid-April (Fig. 9). The simulated anchovy egg production peaks abruptly in May-June and then decreases gradually until the offset of the spawning period in October.

Data on the spatial distribution of eggs are available only for anchovy (Fig. 10), as egg production surveys

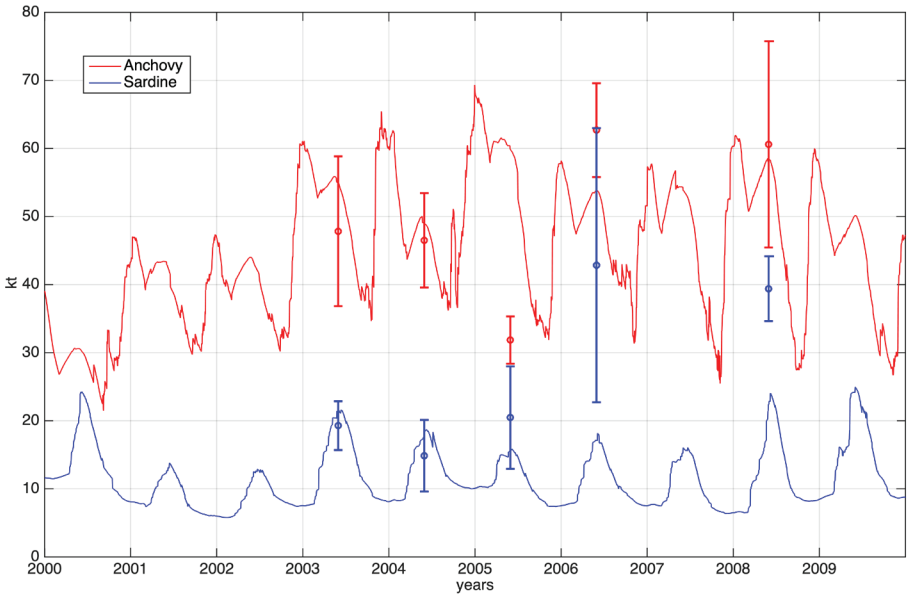

Fig. 7: Simulated biomass (kilotons) evolution (stages: juveniles >80 mm and adults) along with acoustic surveys biomass estimates (red & blue circles ±SD), for the 2000-2008 period.

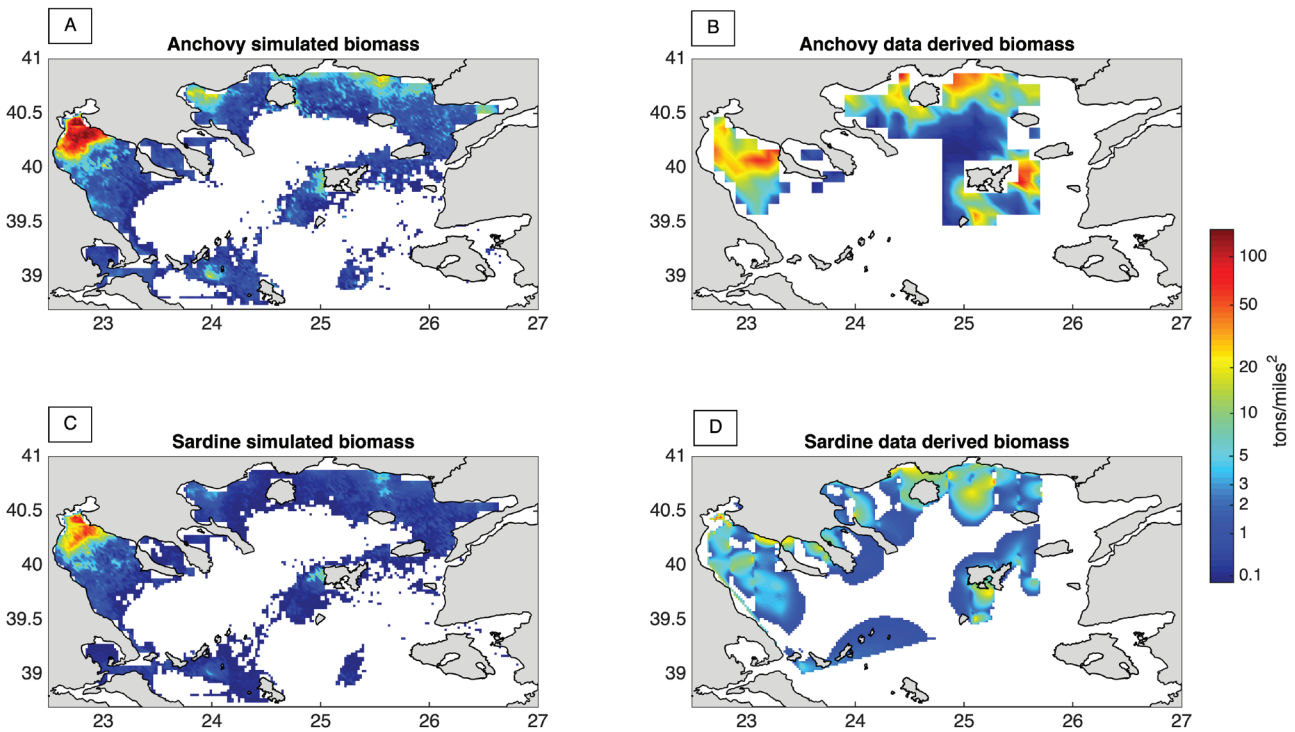

Fig. 8: A) Anchovy and C) Sardine simulated biomass (tons/miles^2) against acoustic surveys (B, D) mean June (2003 - 2008) biomass.

were carried out in summer (Somarakis *et al.,* 2012). The simulated anchovy egg abundance was higher in areas of increased adult biomass (Thermaikos Gulf, Thracian Sea and Strymonikos Gulf, Fig. 10), in agreement with *in situ* data. The model overestimates egg abundance in Thermaikos Gulf, probably due to the overestimation of adult biomass (Fig. 10) and the weak near-surface circulation that results in lower offshore dispersal of eggs (Fig. 3).

Resource competition

In order to investigate species interaction due to resource competition, two additional experiments were performed, with only one species in the model at a time. Results showed that when the two species were separately simulated, their simulated annual mean biomasses were similar: 47kt for anchovy and 42kt for sardine. In the reference simulation, the annual mean biomass was ~45kt for anchovy and 11.5kt for sardine (Table 2). The similar

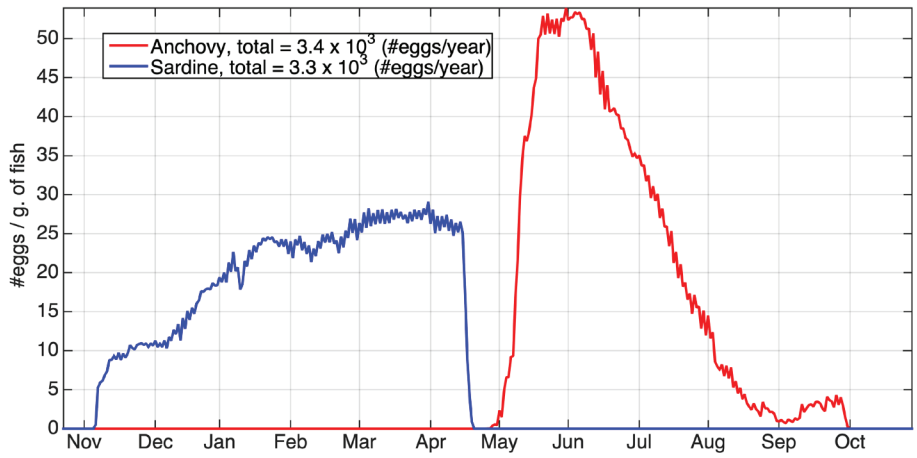

Fig. 9: Mean relative daily egg production (#eggs/g. of fish) for the years 2000-2008.

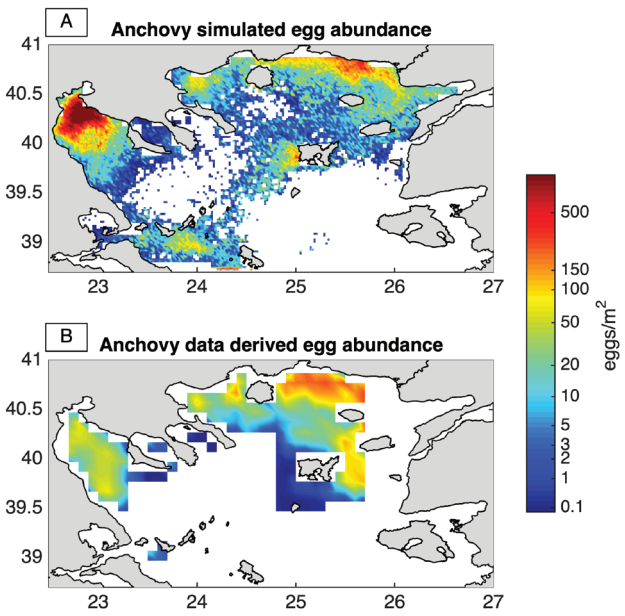

Fig. 10: A) Anchovy mean (June 2003-2008) simulated and B) data derived egg production (eggs/m^2).

simulated mean biomass of the two species implies that the available mesozooplankton concentration probably limits the increase in size of the sardine stock when the anchovy stock is dominant. Competition for limited food is also implied by the relatively increased mesozooplankton biomass in single species simulations (Table 2).

Temperature sensitivity experiments

The effect of temperature increase (dT, +1 °C and +2 °C) on the mean anchovy and sardine biomass is shown in Figure 11. In the two-species simulations, anchovy biomass decreased with increasing temperature (from -37% for dT = +1°C to -64% for dT = +2 °C). In contrast, sardine biomass increased by ~ +5% in both experiments. In single-species simulations, when the temperature increase was applied to all stages (larvae/juveniles and adults, t. on all st.), the biomass of both species decreased (from -25% for dT = +1 °C to -51% for dT = +2 °C for anchovy and from -13% for dT = +1 °C to -32% for dT = +2 °C for sardine). These experiments show that a temperature increase negatively affects both species; however, this is masked in the case of sardine in the two-species simulation due to lower resource competition when anchovy biomass decreases. The negative effect of temperature on fish growth results from the dome-shaped consumption temperature dependence and the (exponential) increase of metabolic costs (mainly respiration) with temperature (see Gkanasos *et al*., 2019, Table 2).

The single species experiments highlight the fact that temperature increases affect anchovy more than sardine. A comparison between the corresponding stages of the species shows that both adult and early stages anchovy are significantly more affected than those of sardine. The anchovy spawning period coincides with maximum yearly sea temperature. Therefore, the high energetic demands of anchovy adults during this period increase even more due to the temperature increase, thus affecting somatic condition and subsequent egg production. The period of anchovy larvae occurrence also partially coincides with maximum annual temperature, which means that these stages are more affected by the temperature increase compared to those of sardine.

Climatic scenarios

In the future climate scenario, sea surface temperature (SST) increased by +1.12 °C on average and sea surface salinity (SSS) increased by +0.09 psu, resulting in increased stratification (indicated by a ~6% decrease in the mixed layer depth). The latter led to a decrease in phytoplankton biomass (-4.6%), followed by a decrease in microzooplankton (-6%) and mesozooplankton (-6.9%) biomass (Fig. 12 and Table 3). These results are derived from a biogeochemical model simulation without the fish model, since the simulated microzooplankton (prey of larvae) and particularly mesozooplankton (prey of late

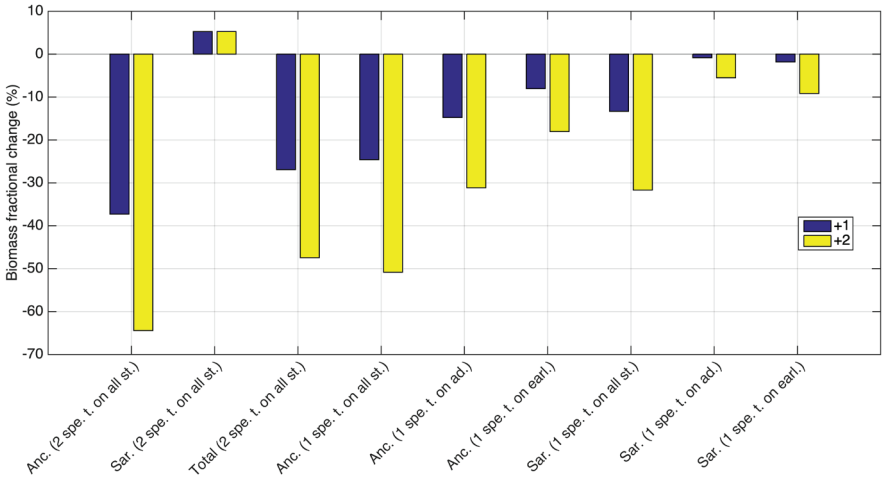

Fig. 11: Temperature effect on biomass. Experiment abbreviations: Anchovy: Anc., Sardine: Sar., Both species (2 spe.), or single species (1 spe.), with temperature effect applied on early stages (t. on earl.), on adult stages (t. on ad.), or on all stages (t. on all st.).

larvae, juveniles and adults) biomasses are significantly affected by total fish biomass and any change would be masked. River and BSW discharge and nutrient inputs remained the same in the present/future simulations.

The temperature increase and zooplankton reduction resulted in a significant decrease (-57%) of anchovy biomass in the "future" while sardine biomass increased by 33% (Table 3). When the two species were simulated separately (not sharing the same resources), both anchovy and sardine biomass decreased (-60% and -51%, respectively). In the two-species simulation, sardine annual mean biomass (44 kt) was higher than anchovy (25 kt), suggesting that environmental changes may lead to a regime shift between the two species in the N. Aegean. To further investigate this, we compared temperature and zooplankton biomass change in the future climate (Table 3) during the critical spawning and larval growth period for anchovy (May-October) and sardine (November-April). The temperature increase and food reduction during May-October were significantly higher, compared to the November-April period. Therefore, anchovy was confronted with more adverse conditions (+135 °C temperature increase and 8-10% food reduction) during its spawning period, compared to sardine (+0.89 °C temperature increase and 3.3-3.7% food reduction), which probably led to the simulated dominance of the latter under future climate conditions.

Discussion

The well-documented long-term environmental changes in the Mediterranean (Skliris *et al*., 2011b; Iona *et al*., 2018) combined with the declining trend, in recent years, of most anchovy and sardine stocks (Tsikliras *et al.,* 2015) point to the necessity of an effective management scheme for small pelagic fish. To this end, it is most important to understand the factors that regulate their abundance, under changing climate conditions, using numerical models. In this study, a three-dimensional IBM model describing the full life cycle of anchovy and sardine in the North Aegean Sea, based on an existing one-dimensional model (Gkanasos *et al*., 2019), was developed. The new 3-D model is two-way coupled with a 3-D LTL that provides the prey (microzooplankton, mesozooplankton) and physical properties (temperature,

Table 3. Biomass and simulated variables alterations for the two periods.

	1980-2000	2080-2100	Future – Present		
			Annual	Nov. - Apr.	May - Oct.
SST (°C)	18.61	19.73	+1.12	+0.89	+1.35
Salinity (psu)	36.44	36.53	+0.09	+0.07	+0.11
Microzooplankton	6.9 (mgC/m^3)	6.55(mgC/m^3)	-6%	-3.7%	-8.3%
Mesozooplankton	8.71 (mgC/m^3)	8.17(mgC/m^3)	-6.9%	-3.3%	-10.4%
Biomasses (kt)	Anc.: 59.5 sar.: 33	Anc.: 25, sar.: 44	Anc.: -57%, sar.:+33%		
2 spe.	81	32	-60%		
1 spe (anchovy)	89	44	-51%		
1 spe (sardine)					

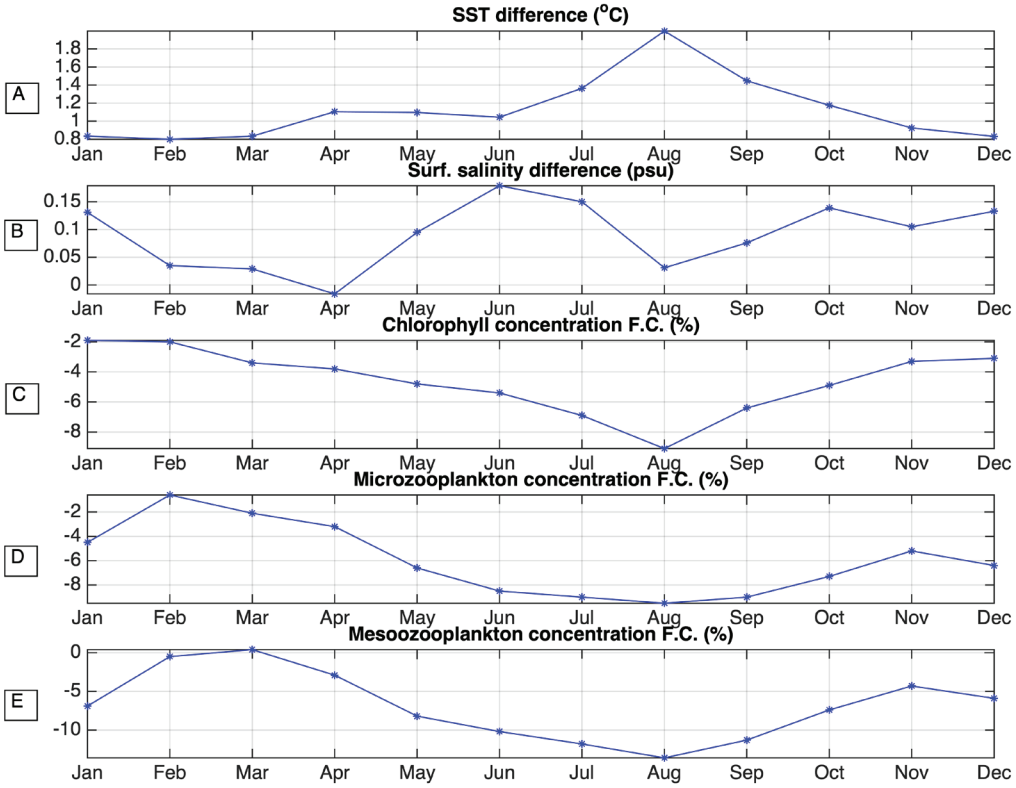

Fig. 12: Simulated mean A) SST (°C) and B) SSS (psu) difference (Future - Present) and C) Chlorophyll, D) Microzooplankton and E) Mesozooplankton fractional change (Future/Present - 1).

currents) of the fish habitat.

The results of this modelling reveal reasonable agreement with field data collected during 2003-2008. Simulated somatic growth (Fig. 6) points to a noticeable difference between the simulated adult weight evolution of the two species in summer, with anchovy weight increasing less compared to sardine. This is mainly due to the fact that anchovy spawns during spring/summer, thus channelling a significant percentage of the energy stored during winter/spring to reproduction, instead of somatic growth. The evolution of modelled anchovy biomass (Fig. 7) reproduced the observed interannual variability during the reference period. However, sardine simulated biomass was relatively stable and did not project the biomass increase indicated by the field data. Simulated biomass (Fig. 8) and the spatial distribution of eggs (Fig. 10) show high concentrations in the more productive coastal areas influenced by rivers (Thermaikos and Strymonikos Gulf, Thracian Sea) and along the BSW pathway, in good agreement with the data from acoustic and egg surveys.

Sensitivity experiments revealed an important effect of resource competition, with both anchovy and sardine achieving similar biomasses in single-species simulations (see Table 2). The fact that identical natural mortalities are used for both species and that their egg production is linked to available resources may partly explain why the two species eventually exhibit similar biomasses. However, when the two species share the same resources and anchovy is the dominant species, the high biomass of anchovy prevents the increase of the sardine stock. Sardine appears to benefit significantly from a decrease in anchovy biomass and is highly dependent on the food resources limitation in the area due to the presence of anchovy. This suggests that anchovy is currently better acclimatized in the N. Aegean, which is supported by an additional simulation using inverted initial biomasses, where the outcome was similar to the reference simulation, i.e., higher anchovy biomass.

As fishing pressure on the two species is similar in the N. Aegean and annual egg production (per fish weight) is comparable, anchovy dominance might be attributed to the difference between the larval growth rate of the two species. Larval growth data (Fig. 5), show that anchovy larvae have higher growth rates (summer) compared to sardine larvae (winter). Moreover, among anchovy larvae (Schismenou *et al.,* 2013), those captured during winter exhibit significantly lower mean growth rate (0.63 mm d^{-1}) compared to those captured in summer (0.8 mm d^{-1}). Sardine larval growth is also positively correlated with temperature (Schismenou *et al*., 2016). Faster growth and smaller transformation length in anchovy (42 mm vs 50 mm in sardine) could lead to lower cumulative larval mortality and, consequently, increased recruitment (Somarakis *et al*., 2019).

Temperature sensitivity experiments (Fig. 11) showed that both species are negatively affected by an increase in temperature (single-species simulations). However, anchovy biomass is reduced more drastically due to the higher energy demands in summer combined with reduced prey availability for both adults (poor somatic condition and egg production) and larvae (slower growth). This is not the case for sardine that spawns during winter.

In the two-species simulations, sardine appears to benefit from a decrease in anchovy biomass due to resource competition, showing a slight increase with temperature.

There are different and sometimes controversial findings in the literature (e.g., Tzanatos *et al*., 2013; Jardim *et al*., 2014; Piroddi *et al.,* 2017; Nakayama *et al*., 2018) regarding the effect of temperature on anchovy and sardine. Tzanatos *et al.* (2013) and Nakayama *et al*. (2018) suggest a positive correlation of SST with anchovy, while Jardim *et al*. (2014) and Piroddi *et al.* (2017) indicate a simultaneous drop in the biomass of both species with increasing temperature. However, these findings derive mainly from analyses of historical time series of fisheries and temperature data. In this study, we investigate future climate-driven changes on fish, considering anchovy and sardine biology and ecology as well as their interaction through resource competition. Takasuka *et al.* (2007), present a possible explanation of the regime shifts between anchovy and sardine in the North Pacific, using the "optimal growth temperature hypothesis". Briefly, biomass alterations are due to ambient temperature deviations from the optimal growth temperature of larvae; it differs between anchovy and sardine.

In both species, fish growth at each stage is regulated primarily by the half-saturation parameters of consumption (see Table 1) that are tuned in order to obtain a best fit with the available growth data (Figs 4 and 5). Thus, a relatively higher half-saturation coefficient is adopted for sardine larvae, to reproduce the observed lower growth during the autumn-winter period. Indicatively, sardine half-saturation parameters for the early and late larval stages are 42% and 88% higher, respectively, compared to those fitted for anchovy.

In the model, the effect of temperature is largely determined by the adopted optimum consumption temperatures (cto) for each life stage and were calculated based on their average ambient temperatures. Due to the lack of sufficient data on the effect of temperature on energy rates, the same temperature dependence is adopted for anchovy and sardine based on the similarities of the two species, except for the optimum temperatures for food consumption by the larvae (see Table 1). These are assumed to be close to their mean ambient temperatures during the two different seasons (autumn-winter for sardine, spring-summer for anchovy). Thus, if the current average ambient temperature is lower than the selected cto, a temperature increase will have a positive effect on consumption and growth up to the selected cto. Temperatures above that turning point will result in a significant decrease of energetic functions, since consumption drops more abruptly after the cto value. Therefore, the choice of cto for each species/stage may lead to different results, which might be magnified due to resource competition between the two species.

Finally, the impact of climate change on the two-species biomass was investigated by means of simulations adopting present (1980-2000) and future (2080-2100) climatic conditions under the IPCC-A1B scenario. The different responses of the species are partly attributed to resource competition, as sardine benefits from anchovy biomass reduction. Single-species simulations showed that the biomass of both species will decline; however, the decrease in sardine biomass will be lower. This is because the increase in temperature (%) and zooplankton reduction are higher during anchovy egg production and the larval growth period (see Table 3). Therefore, the pressure of climate change on anchovy is predicted to be greater. When the two species coexist, due to resource competition, sardine is expected to become the dominant species.

The projected results for anchovy and sardine biomass in the future scenario are similar to those in the temperature sensitivity experiments. The projected climate change warming is roughly comparable with the dT=+1^{o}C temperature increase experiments, indicating an anchovy biomass decrease of -37% and a sardine biomass increase of +5% in the two-species simulation (Fig. 11). These changes were amplified (anchovy -57%, sardine +33%) in the future climate scenario due to the differential decrease of food availability during the spawning periods of the two species combined with resource competition that favoured sardine. In the single species simulations (Table 3), the reduction of both anchovy (-60%) and sardine (-51%) biomass in the future climate scenario is significantly greater compared to the -25% and -13% reductions in the temperature sensitivity scenario. This can be partly attributed to the zooplankton decrease. Another factor that must be considered is the longer duration (20 years) of the future climate scenarios, resulting in a magnified effect, compared to the temperature sensitivity experiment (10 years). Changes similar to the above, i.e., temperature increase and zooplankton decrease have been described by Hermann *et al*. (2014) and Hidalgo *et al*. (2018) in their studies on the effects of climate change in the Mediterranean Sea. They concluded that these changes will result in an overall species decline.

Future work will entail an extension of this analysis to the entire Mediterranean Sea, incorporating specific species parameterization for each sub-area (e.g., Adriatic Sea, Gulf of Lions, Aegean Sea). Differences between the Eastern and Western part of the basin will be studied and connections to world climatic oscillations, such as the Atlantic Multidecadal Oscillation (AMO) and North Atlantic Oscillation (NAO) will be investigated.

Acknowledgements

This work was financially supported by the EC H2020 CLAIM project (grant agreement no. 774586) and the General Secretariat for Research and Technology (GSRT) and the Hellenic Foundation for Research and Innovation (HFRI) under project CLIMAFISH – 'CLIMAte change and FISHeries impacts on small pelagic fish: dynamic, spatially explicit models in the service of the ecosystem-based fisheries management' within the framework of the "1st Call for the support of Postdoctoral Researchers".

References

Androulidakis, Y., Kourafalou, V., 2011. Evolution of a buoyant outflow in the presence of complex topography: The Dardanelles plume (North Aegean Sea). *Journal of Geophysical Research*, 116 (C4).

Antonakakis, K., Giannoulaki, M., Machias, A., Somarakis, S., Sanchez, S. *et al*., 2011. Assessment of the sardine (*Sardina pilchardus* Walbaum, 1792) fishery in the eastern Mediterranean basin (North Aegean Sea). *Mediterranean Marine Science*, 12 (2), 333.

Baretta, J., Ebenhöh, W., Ruardij, P., 1995. The European regional seas ecosystem model, a complex marine ecosystem model. *Netherlands Journal of Sea Research*, 33 (3-4), 233-246.

Blumberg, A., Mellor, G., 1983. Diagnostic and prognostic numerical circulation studies of the South Atlantic Bight. *Journal of Geophysical Research: Oceans,* 88 (C8), 4579-4592.

Brosset, P., Ménard, F., Fromentin, J., Bonhommeau, S., Ulses, C. *et al.*, 2015. Influence of environmental variability and age on the body condition of small pelagic fish in the Gulf of Lions. *Marine Ecology Progress Series*, 529, 219-231.

Christensen, J.H., Bøssing Christensen, O., Lopez, P., van Meijgaard, E., Botzet, M., 1996. The HIRHAM4 Regional Atmospheric Climate Model. *Scientific Report,* 96-4, Danish Meteorological Institute.

Chust, G., Allen, J.I., Bopp, L., Schrum, C., Holt, J., *et al.*, 2014. Biomass changes and trophic amplification of plankton in a warmer ocean, *Global Change Biology,* 20 (7), 2124-2139.

Frangoulis, C., Psarra, S., Zervakis, V., Meador, T., Mara, P. *et al.*, 2010. Connecting export fluxes to plankton food-web efficiency in the Black Sea waters inflowing into the Mediterranean Sea. *Journal of Plankton Research,* 32 (8), 1203-1216.

Fréon, P., Cury, P., Shannon, L., Roy, C., 2005. Sustainable exploitation of small pelagic fish stocks challenged by environmental and ecosystem changes. *Bulletin of Marine Science*, 76 (2), 385-462.

Ganias, K., Somarakis, S., Nunes, C., 2014. Reproductive potential. In: Biology and Ecology of Sardines and Anchovies. *CRC Press*, Taylor & Francis Group, Boca Raton, 79-121.

Gatti, P., Petitgas, P., Huret, M., 2017. Comparing biological traits of anchovy and sardine in the Bay of Biscay: A modelling approach with the Dynamic Energy Budget. *Ecological Modelling*, 348, 93-109.

Giannoulaki, M., Machias, A., Somarakis, S., Tsimenides, N., 2005. The spatial distribution of anchovy and sardine in the northern Aegean Sea in relation to hydrographic regimes. *Belgian Journal of Zoology,* 135 (2), 151.

Giannoulaki, M., Ibaibarriaga, L., Antonakakis, K., Uriarte, A., Machias, A. *et al.* 2014. Applying a two-stage Bayesian dynamic model to a short-lived species, the anchovy in the Aegean Sea (Eastern Mediterranean): Comparison with an integrated catch at age stock assessment model. *Mediterranean Marine Science*, 15 (2), 350-365.

Gkanasos, A., Somarakis, S., Tsiaras, K., Kleftogiannis, D., Giannoulaki, M. *et al.*, 2019. Development, application and evaluation of a 1-D full life cycle anchovy and sardine model for the North Aegean Sea (Eastern Mediterranean). *PloS ONE*, 14 (8).

Gualdi, S., Scoccimarro, E., Navarra, A., 2008. Changes in Tropical Cyclone Activity due to Global Warming: Results from a High-Resolution Coupled General Circulation Model. *Journal of Climate*, 21 (20), 5204-5228.

Herrmann, M., Estournel, C., Adloff, F., Diaz, F., 2014. Impact of climate change on the western Mediterranean Sea pelagic planktonic ecosystem and associated carbon cycle. *Journal of Geophysical Research: Oceans,* 119 (9), 5815-5836.

Hidalgo, M., Mihneva, V., Vasconcellos, M., Bernal, M., 2018. Climate change impacts, vulnerabilities and adaptations: Mediterranean Sea and the Black Sea marine fisheries. In: M. Barange, T. Bahri, M. C. Beveridge, K. Cochrane, S. Funge-Smith & F. Poulain (Eds.), Impacts of Climate Change on Fisheries and Aquaculture: Synthesis of Current Knowledge, Adaptation and Mitigation Options, 139-159. Rome, Italy: *FAO Fisheries and Aquaculture. Technical Paper* No. 627, 628 Pp. FAO.

Huret, M., Petitgas, P., Woillez, M., 2010. Dispersal kernels and their drivers captured with a hydrodynamic model and spatial indices: A case study on anchovy (*Engraulis encrasicolus*) early life stages in the Bay of Biscay. *Progress in Oceanography*, 87 (1-4), 6-17.

Iona, A., Theodorou, A., Sofianos, S., Watelet, S., Troupin, C. *et al.*, 2018. Mediterranean Sea climatic indices: monitoring long-term variability and climate changes. *Earth System Science Data*, 10 (4), 1829-1842.

Jardim, E., Millar, C., Mosqueira, I., Scott, F., Osio, G. *et al*., 2014. What if stock assessment is as simple as a linear model? The a4a initiative. ICES *Journal of Marine Science*, 72 (1), 232-236.

Kalaroni, S., Tsiaras, K., Petihakis, G., Economou-Amilli, A., Triantafyllou, G., 2020. Modelling the mediterranean pelagic ecosystem using the POSEIDON ecological model. Part II: Biological dynamics. *Deep Sea Research Part II*: *Topical Studies in Oceanography*, 171, 104647.

Katara, I., Pierce, G., Illian, J., Scott, B., 2011. Environmental drivers of the anchovy/sardine complex in the Eastern Mediterranean. *Hydrobiologia*, 670 (1), 49-65.

Kokkini, Z., Potiris, M., Kalampokis, A., Zervakis, V., 2014. HF Radar observations of the Dardanelles outflow current in North Eastern Aegean using validated WERA HF radar data. *Mediterranean Marine Science*, 15 (4), 753.

Kourafalou, V., Tsiaras, K., 2007. A nested circulation model for the North Aegean Sea. *Ocean Science*, 3 (1), 1-16.

Morote, E., Olivar, M. P., Villate, F., Uriarte, I., 2010. A comparison of anchovy (*Engraulis encrasicolus*) and sardine (*Sardina pilchardus*) larvae feeding in the Northwest Mediterranean: influence of prey availability and ontogeny. ICES *Journal of Marine Science*, 67, 897-908.

Nakayama, S., Takasuka, A., Ichinokawa, M., Okamura, H., 2018. Climate change and interspecific interactions drive species alternations between anchovy and sardine in the western North Pacific: Detection of causality by convergent cross mapping. *Fisheries Oceanography*, 27 (4), 312-322.

Nikolioudakis, N., Palomera, I., Machias, A., Somarakis, S., 2011. Diel feeding intensity and daily ration of the sardine Sardina pilchardus. *Marine Ecology Progress Series*, 437, 215-228.

Nittis, K., Perivoliotis, L., Korres, G., Tziavos, C., Thanos, I., 2006. Operational monitoring and forecasting for marine

environmental applications in the Aegean Sea. *Environmental Modelling and Software*, 21 (2), 243-257.

Olson, D., Kourafalou, V., Johns, W., Samuels, G., Veneziani, M., 2007. Aegean Surface Circulation from a Satellite-Tracked Drifter Array. *Journal of Physical Oceanography*, 37 (7), 1898-1917.

O'Reilly, J., Maritorena, S., Mitchell, B.G., Siegel, D., Carder, K.L. *et al.*, 1998. Ocean color chlorophyll algorithms for SeaWiFS. *Journal of Geophysical Research: Oceans*, 103 (C11), 24937-24953.

Petihakis, G., Triantafyllou, G., Allen, I., Hoteit, I., Dounas, C., 2002. Modelling the spatial and temporal variability of the Cretan Sea ecosystem. *Journal of Marine Systems*, 36 (3-4), 173-196.

Petihakis, G., Tsiaras, K., Triantafyllou, G., Kalaroni, S., Pollani, A., 2014. Sensitivity of the N. AEGEAN SEA ecosystem to Black Sea Water inputs. *Mediterranean Marine Science*, 15 (4), 790-804.

Piroddi, C., Coll, M., Liquete, C., Macias, D., Greer, K. *et al.*, 2017. Historical changes of the Mediterranean Sea ecosystem: modelling the role and impact of primary productivity and fisheries changes over time. *Scientific Reports*, 7 (1), 1-18.

Polat, C., Tuğrul, S., 1996. Chemical exchange between the mediterranean and black sea via the Turkish straits, CIESM science series. *Bulletin de l'Institut océanographique (Monaco),* 167-186.

Politikos, D., Somarakis, S., Tsiaras, K.P., Giannoulaki, M., Petihakis, G. *et al*. 2015. Simulating anchovy's full life cycle in the northern Aegean Sea (eastern Mediterranean): A coupled hydro-biogeochemical-IBM model. *Progress in Oceanography*, 138, 399-416.

Rose, K.A., Fiechter, J., Curchitser, E.N., Hedstrom, K., Bernal, M. *et al*. 2015. Demonstration of a fully-coupled end-to-end model for small pelagic fish using sardine and anchovy in the California Current. *Progress in Oceanography*, 138, 348-380.

Sánchez-Garrido, J., Werner, F., Fiechter, J., Rose, K., Curchitser, E. *et al.*, 2019. Decadal-scale variability of sardine and anchovy simulated with an end-to-end coupled model of the Canary Current ecosystem. *Progress in Oceanography*, 171, 212-230.

Sarmiento, J., Hughes, T., Stouffer, R., Manabe, S., 1998. Simulated response of the ocean carbon cycle to anthropogenic climate warming. *Nature*, 393 (6682), 245-249.

Scheffer, M., Baveco, J.M., DeAngelis, D.L., Rose, K.A., van Nes, E.H., 1995. Super-individuals: a simple solution for modelling, large populations on an individual basis. *Ecological Modelling,* 80 (2-3), 161-170.

Schismenou, E., 2012. *Modern approaches in biology and ecology of reproduction and growth of anchovy (*Engraulis Encrasicolus*) in the North Aegean Sea*. *PhD thesis*, University of Crete, Greece.

Schismenou, E., Tsiaras, K., Kourepini, M.I., Lefkaditou, E., Triantafyllou, G. *et al.*, 2013. Seasonal changes in growth and condition of anchovy late larvae explained with a hydrodynamic-biogeochemical model simulation. *Marine Ecology Progress Series,* 478, 197-209.

Schismenou, E., Palmer, M., Giannoulaki, M., Alvarez, I., Tsiaras, K. *et al*. 2016. Seasonal changes in otolith increment width trajectories and the effect of temperature on the daily growth rate of young sardines. *Fisheries Oceanography*, 25 (4), 362-372.

Siokou-Frangou, I., Bianchi, M., Christaki, U., Christou, E.D., Giannakourou, A. *et al.*, 2002. Carbon flow in the planktonic food web along a gradient of oligotrophy in the Aegean Sea (Mediterranean Sea). *Journal of Marine Systems*, 33, 335-353.

Skliris, N., Sofianos, S., Gkanasos, A., Axaopoulos, P., Mantziafou, A. *et al.*, 2011a. Long-term sea surface temperature variability in the Aegean Sea. *Advances in Oceanography and Limnology,* 2 (2), 125-139.

Skliris, N., Sofianos, S., Gkanasos, A., Mantziafou, A., Vervatis, V. *et al*., 2011b. Decadal scale variability of sea surface temperature in the Mediterranean Sea in relation to atmospheric variability. *Ocean Dynamics*, 62 (1), 13-30.

Skoulikidis, N.Th., 2009. The environmental state of rivers in the Balkans-A review within the DPSIR framework. *Science of the Total Environment*, 407 (8), 2501-2516.

Somarakis S., 1999. *Ichthyoplankton of the NE Aegean with emphasis on anchovy,* Engraulis Encrasicolus *(Linnaeus, 1758)* (June 1993, 1994, 1995, 1996). PhD thesis, University of Crete.

Somarakis, S., Schismenou, E., Siapatis, A., Giannoulaki, M., Kallianiotis, A. *et al.*, 2012. High variability in the Daily Egg Production Method parameters of an eastern Mediterranean anchovy stock: Influence of environmental factors, fish condition and population density. *Fisheries Research*, 117-118, 12-21.

Somarakis, S., Tsoukali, S., Giannoulaki, M., Schismenou, E., Nikolioudakis, N., 2019. Spawning stock, egg production and larval survival in relation to small pelagic fish recruitment. *Marine Ecology Progress Series*, 617, 113-136.

Stergiou, K., Somarakis, S., Triantafyllou, G., Tsiaras, K., Giannoulaki, M. *et al.*, 2016. Trends in productivity and biomass yields in the Mediterranean Sea Large Marine Ecosystem during climate change. *Environmental Development*, 17, 57-74.

Takasuka, A., Oozeki, Y., Aoki, I., 2007. Optimal growth temperature hypothesis: Why do anchovy flourish and sardine collapse or vice versa under the same ocean regime? *Journal of Fisheries and Aquatic Sciences*, 64 (5), 768-776.

Tuğrul, S., Besiktepe, S.T., Salihoglou, I., 2002. Nutrient exchange fluxes between the Aegean and Black seas through the marmara sea. *Mediterranean Marine Science*, 3 (1), 33-42.

Travers, M., Shin, Y.-J., Jennings, S., Cury, P., 2007. Towards end-to-end models for investigating the effects of climate and fishing in marine ecosystems. *Progress in Oceanography,* 75 (4), 751-770.

Tsiaras, K., Kourafalou, V., Raitsos, D., Triantafyllou, G., Petihakis, G. *et al.*, 2012. Inter-annual productivity variability in the North Aegean Sea: Influence of thermohaline circulation during the Eastern Mediterranean Transient. *Journal of Marine Systems*, 96-97, 72-81.

Tsiaras, K., Petihakis G., Kourafalou, V., Triantafyllou G., 2014. Impact of the river nutrient load variability on the N. Aegean ecosystem functioning over the last decades. *Journal of sea research*, 86, 97-109.

Tsikliras, A.C., 2007. Thermal threshold of the onset of maturation in clupeid fishes using quotient analysis. *Rapport du*

Congrès de la Commission Internationale pour l'Exploration Scientifique de la Mer Méditerranée, 38, 623.

Tsikliras, A., Dinouli, A., Tsiros, V., Tsalkou, E., 2015. The Mediterranean and Black Sea Fisheries at Risk from Overexploitation. *PloS ONE,* 10 (3), e0121188.

Tzanatos, E., Raitsos, D., Triantafyllou, G., Somarakis, S., Tsonis, A., 2013. Indications of a climate effect on Mediterranean fisheries. *Climatic Change*, 122 (1-2), 41-54.

Vilibić, I., Čikeš Keč, V., Zorica, B., Šepić, J., Matijević, S. *et al.*, 2016. Hydrographic conditions driving sardine and anchovy populations in a land-locked sea. *Mediterranean Marine Science,* 17 (1), 1-2.

Voulgaridou, P., Stergiou, K.I., 2003. Trends in various biological parameters of the European sardine, Sardina pilchardus (Walbaum, 1792), in the Eastern Mediterranean Sea. *Scientia Marina,* 67, 269-280.

Zervakis, V., Georgopoulos, D., 2002. Hydrology and circulation in the North Aegean (eastern Mediterranean) throughout 1997 and 1998. *Mediterranean Marine Science*, 3 (1), 5-19.